

Report

The 4<sup>th</sup> Annual WAMIT Consortium Meeting

October 8-9, 2003

Woods Hole, Massachusetts

## Agenda for 4<sup>th</sup> Annual WAMIT Meeting at Swope Center, Woods Hole, MA

October 8:

8:00AM: Breakfast

9:00AM: Welcome

9:15AM: "Time Domain Impulse Response Functions"

J. N. Newman, WAMIT

9:45AM: "Dipole Panels and Patches in WAMIT"

C.-H. Lee, WAMIT

10:15AM: "Updates in Version 6.2"

C.-H. Lee, WAMIT

10:45AM: Break

11:00AM: "Application of generalized modes for the simulation of free surface patches in multiple body interactions"

J. N. Newman, WAMIT

11:30AM: "Integration of Second-Order Forcing in the Higher-Order Method"

C.-H. Lee, WAMIT

12:00PM: Lunch

1:30PM: "Numerical Prediction of Hydrodynamic Damping using a Viscous Solver Embedded in a Potential Code"

T. Kendon, JMR Graham and SJ Sherwin, Imperial College, UK

2:10PM: "Effect of Ocean Turbulence on Drag/Lift Forces and VIV of Offshore Structures - Generation of Turbulent Velocity Fields For Use In CFD Simulations" R. Mercier, OTRC

2:40PM: Break

3:00PM: "Steep wave effects around multicolumn structure"

P. Teigen, Statoil & Niedzwecki, OTRC

3:30PM: "2nd order diffraction vs. fully non linear calculations -- the Statoil workshop in retrospect"

P. Teigen, Statoil

5:30PM: Mixer and Dinner

October 9:

8:00AM: Breakfast

9:00AM: "Computation of the fluid velocity"  
C.-H. Lee, WAMIT

9:30AM: "Recent updates in the pFFT-method in WAMIT"  
C.-H. Lee, WAMIT

10:00AM: Technical Plans for 2004"

10:30AM: Break

10:50AM: Business meeting

12:00AM: Lunch

## Contents

1. Time Domain Impulse Response Functions
2. Dipole Panels and Patches in WAMIT
3. Updates in Version 6.2
4. Application of generalized modes for the simulation of free surface patches in multiple body interactions
5. Integration of Second-Order Forcing in the Higher-Order Method
6. Computation of the fluid velocity
7. Recent updates in the pFFT-method in WAMIT
8. Current Participants
9. Appendices

F2T Version 3 User Manual – J. N. Newman

Computation of wave effects using the panel methods – C.-H. Lee and J. N. Newman  
(To appear in 'Numerical Modeling in Fluid-Structure Interaction.' WTI Press)

Low-frequency resonance of moon-pools – J. N. Newman

(18<sup>th</sup> Workshop on Water Waves and Floating Bodies – Le Croisic, France)

# Time-Domain Impulse Response Functions

By J. N. Newman

The objective is to develop a robust utility which can be used for general purposes, based on standard WAMIT outputs. A preliminary version of the utility F2T was described last year. It has now been extended and updated, in conjunction with WAMIT V6.2. F2T now accepts as input all first-order Options 1-7 for all possible values of input parameters, and outputs the corresponding IRFs in the time domain. Extensions in V6.2 make it easier to generate the required inputs for F2T. (Zero, infinite wave periods can be included in the main run.)

# Inputs from WAMIT:

- Numeric output files for any combination of Options 1-7 , arbitrary numbers of modes, generalized modes, bodies, etc.
- This data must be evaluated at a large set of uniformly spaced frequencies (including zero and infinity, if radiation modes are physically relevant to the problem)

# Outputs from F2T

- Similar files to the numeric output files from WAMIT with PERIOD replaced by TIME in uniformly spaced time steps, and frequency-domain coefficients replaced by their Fourier transforms.
- Duplicative files with impulse response functions tabulated in a format more suitable for use.



# Radiation IRFs (Option 1)

(also applies for the radiation modes in options 5,6,7)

$$A_{ij}(\omega) - A_{ij}(\infty) = \int_0^{\infty} L_{ij}(t) \cos \omega t dt$$

$$B_{ij}(\omega) = \omega \int_0^{\infty} L_{ij}(t) \sin \omega t dt$$

$$L_{ij}(t) = \frac{2}{\pi} \int_0^{\infty} [A_{ij}(\omega) - A_{ij}(\infty)] \cos \omega t d\omega$$

$$L_{ij}(t) = \frac{2}{\pi} \int_0^{\infty} \frac{B_{ij}(\omega)}{\omega} \sin \omega t d\omega$$

# Diffraction IRFs (Options 2,3,4)

(also applies for the diffraction modes in options 5,6,7)

$$X_i(\omega) = \int_{-\infty}^{\infty} K_i(t) e^{-i\omega t} dt$$

$$2\pi K_i(t) = \int_{-\infty}^{\infty} X_i(\omega) e^{i\omega t} d\omega$$

$$X_i(-\omega) = X_i^*(\omega)$$

$$K_i(t) = \frac{1}{\pi} \int_0^{\infty} [\operatorname{Re}(X_i) \cos \omega t - \operatorname{Im}(X_i) \sin \omega t] d\omega$$

# Pros and Cons of WAMIT+F2T vs. TiMIT

- Pro: availability of WAMIT options including finite depth, higher-order analysis, MultiSurf or Geomxact geometry  
Faster run times for complex structures and/or large-time simulations. **Can be used for options 5,6,7.**
- Con: no current or forward speed  
no nonlinear hydrostatics

# Numerical implementation

- Filon integration is used for robustness
- Inputs must be a set of uniformly spaced frequencies
- Truncation correction for high-frequency contribution to integrals is based on the total integral of the damping coefficient  
(changed from last year)
- Theory and use are documented in F2T.PDF (see Appendix)

---

# Dipole panels and patches in WAMIT

---

# Equations

The body surface is assumed to consist of two parts, a conventional portion  $S_b$  with nonzero thickness and another portion  $S_d$  of zero thickness, designated as the dipole surface. In this case the potential on  $S_b$  or in the interior of the fluid can be represented in the form

$$\left(\frac{2\pi}{4\pi}\right)\phi(\mathbf{x}) + \iint_{S_b} \phi G_{n_\xi} dS_\xi + \iint_{S_d} \Delta\phi G_{n_\xi} dS_\xi = \iint_{S_b} \phi_{n_\xi} G dS_\xi, \quad (1)$$

where  $\Delta\phi$  is the difference of the potential on the two opposite sides of  $S_d$ . When  $\mathbf{x}$  is on the dipole surface  $S_d$ , the normal derivative of (1) can be used to derive the equation

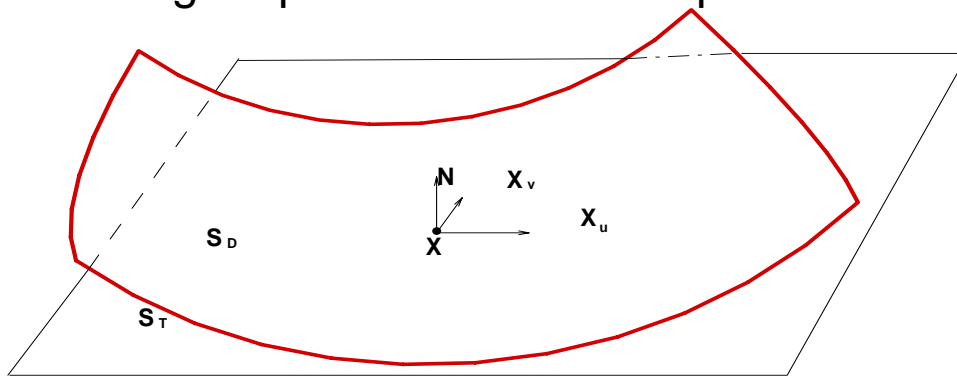
$$\iint_{S_b} \phi G_{n_\xi n_x} dS_\xi + \iint_{S_d} \Delta\phi G_{n_\xi n_x} dS_\xi = -4\pi\phi_n(\mathbf{x}) + \iint_{S_b} \phi_{n_\xi} G_{n_x} dS_\xi. \quad (2)$$

An appropriate pair of coupled integral equations for this problem follow by using (1) for points on  $S_b$  and (2) for points on  $S_d$  to solve simultaneously for the unknowns  $\phi$  on  $S_b$  and  $\Delta\phi$  on  $S_d$ . In the diffraction problem the right-hand sides of these equations are replaced by  $4\pi\phi_I(\mathbf{x})$  and  $4\pi\phi_{In}(\mathbf{x})$ .

# Evaluation of the hyper-singular integral due to the double normal derivative

Low-order : Application of the Biot-Savart law over flat panels

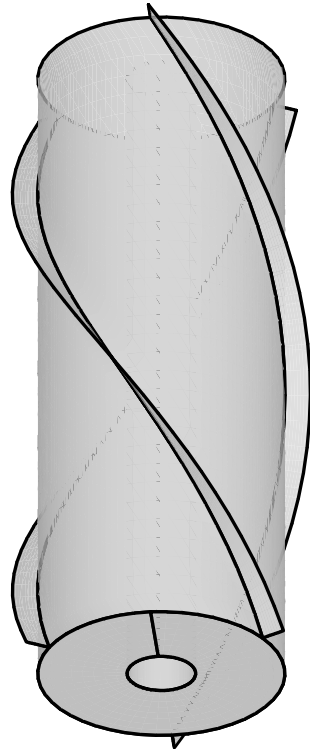
Higher-order : Tangent plane + Numerical quadrature



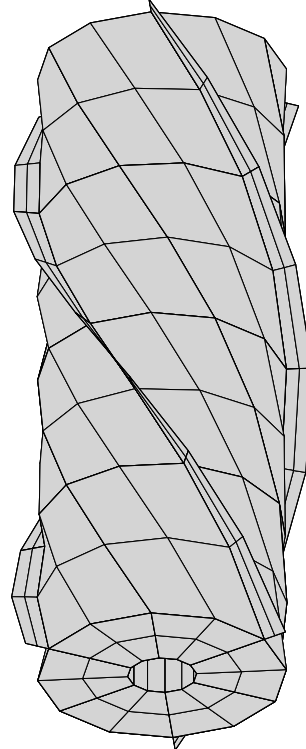
$$\iint_{S_D} \left(\frac{1}{r}\right)_{n_\xi n_x} dS = \iint \left(\frac{1}{r_{S_D}}\right)_{n_\xi n_x} - \left(\frac{1}{r_{S_T}}\right)_{n_\xi n_x} dudv + \iint_{S_T} \left(\frac{1}{r}\right)_{n_\xi n_x} dS$$

$dX/du = \text{constant}$  is assumed on the tangent plane

# Application 1



(a)

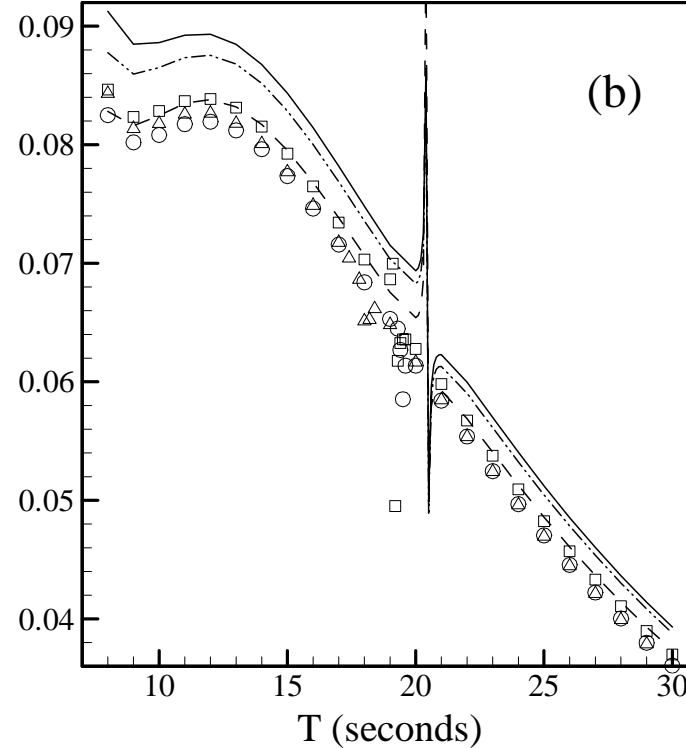
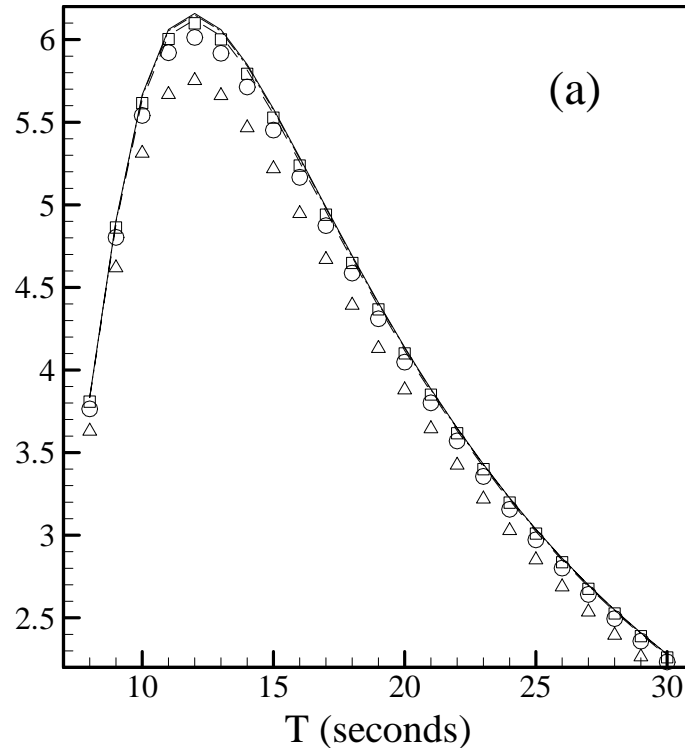


(b)

Input geometry for the higher-order method (a) and low-order method (b)  
(SPAR (IGDEF=-12) in GEOMXACT of V6.2 )



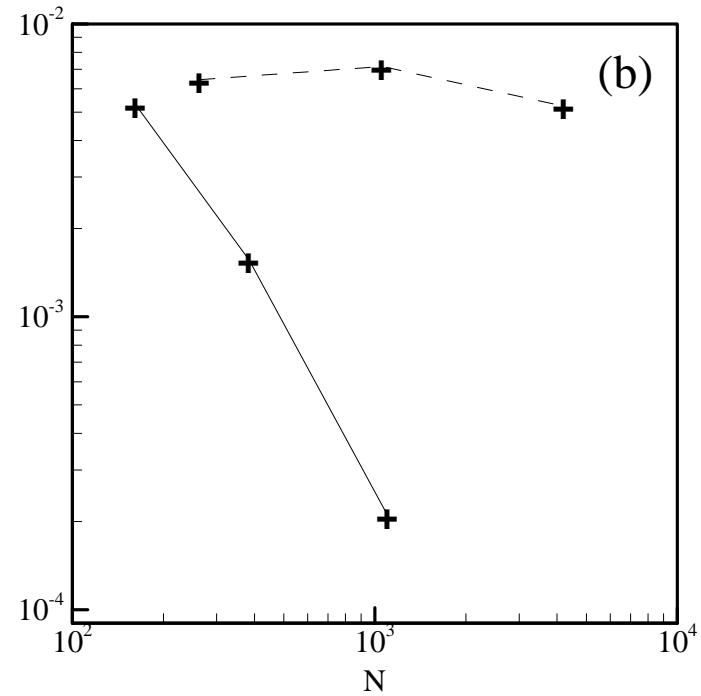
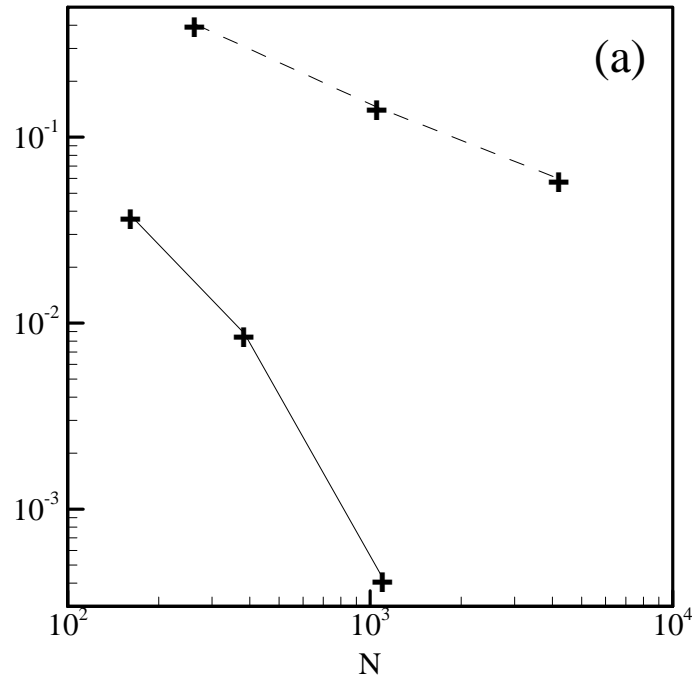
# Surge force (a) and Yaw moment (b)



Lines: higher-order method (N=162, 384 and 1104)

Symbols: low-order method (N=414, 1656 and 6264)

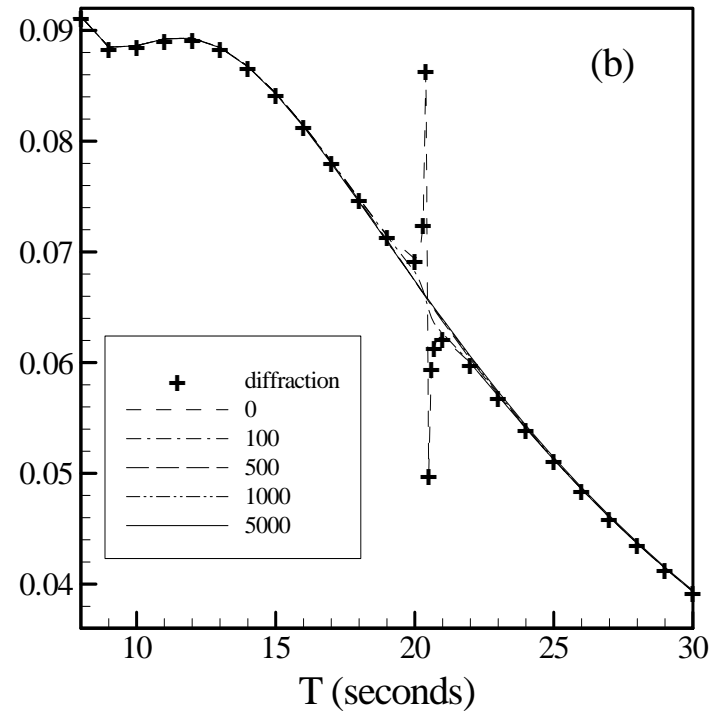
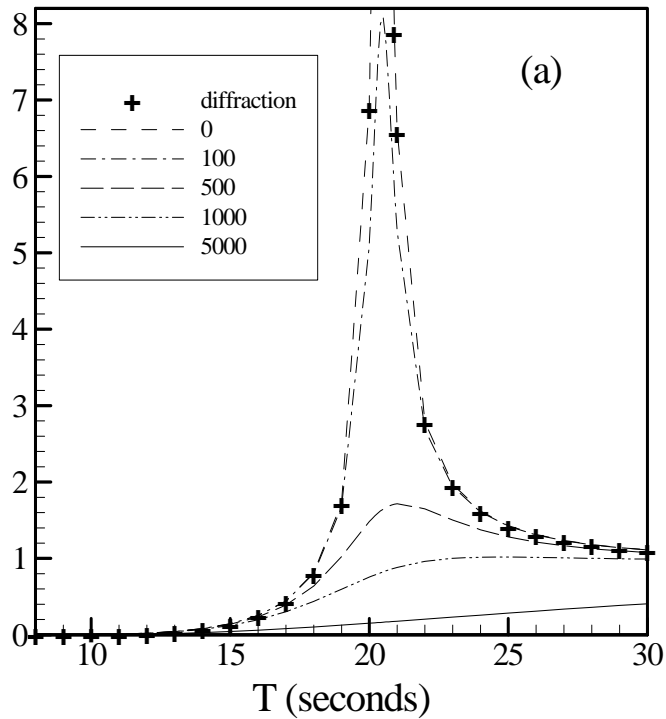
# Error at T=12 seconds



Surge force (a) and Yaw moment (b)

Dashed lines: low order    Solid lines: higher order

# Moonpool resonance

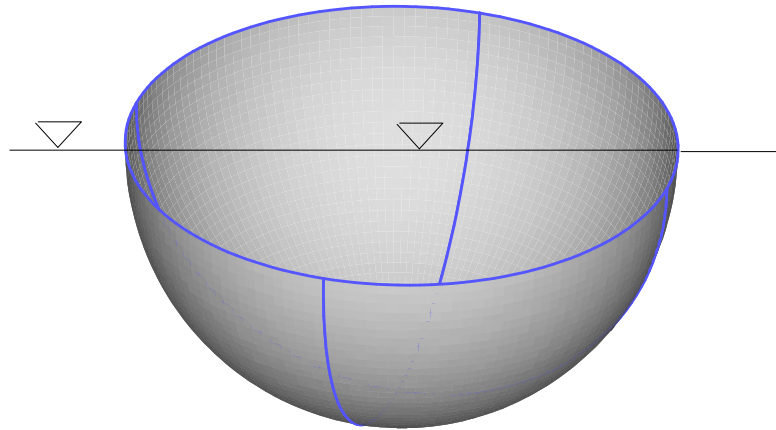


Free surface elevation (a) and yaw moment (b)  
With various damping applied to the piston mode

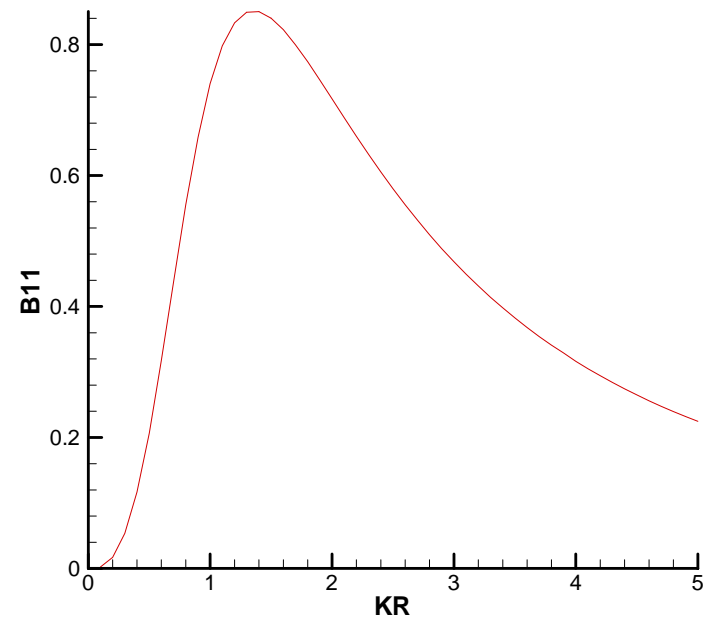
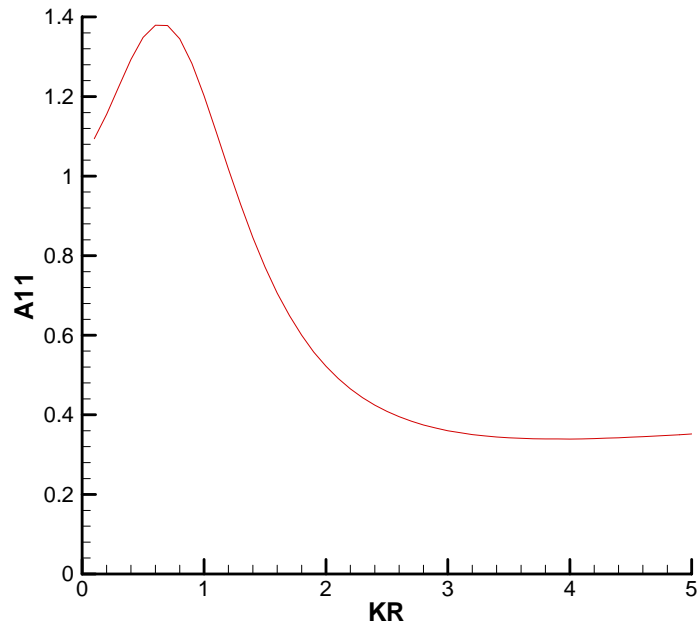
---

# Application 2

Two regions divided by thin surfaces can be analysed using dipole panels/patches.

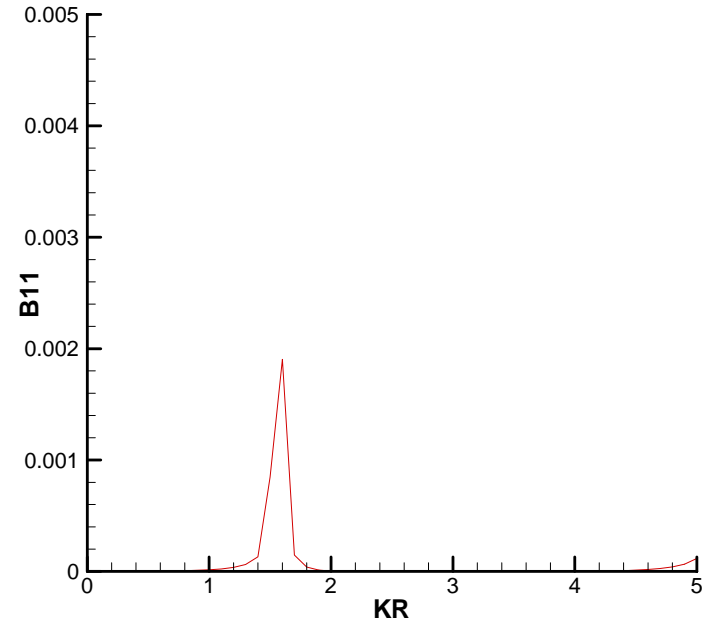
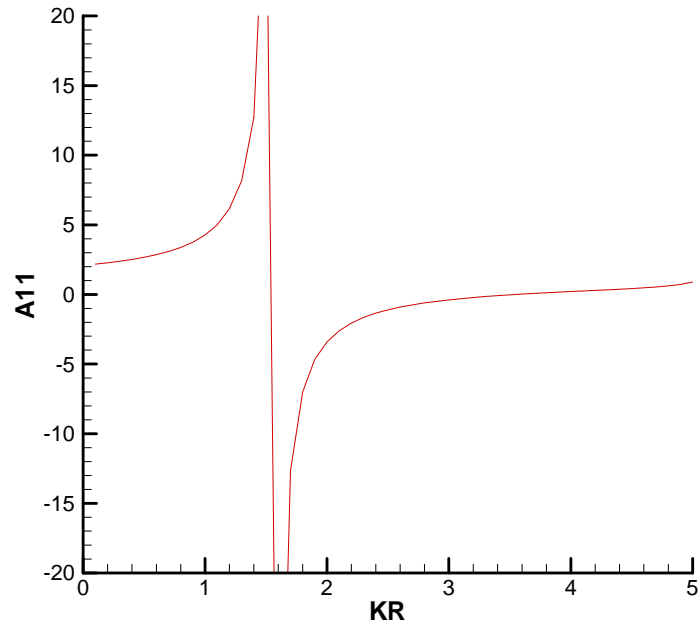


# Surge External (Normal into the body)



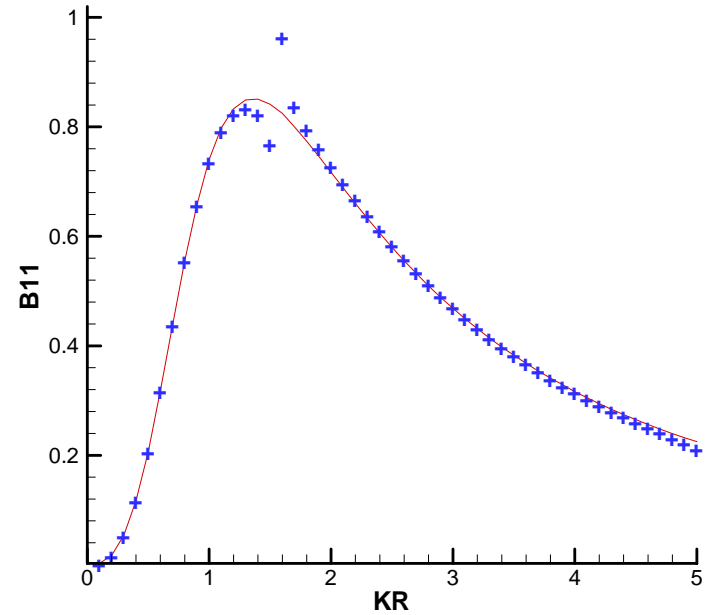
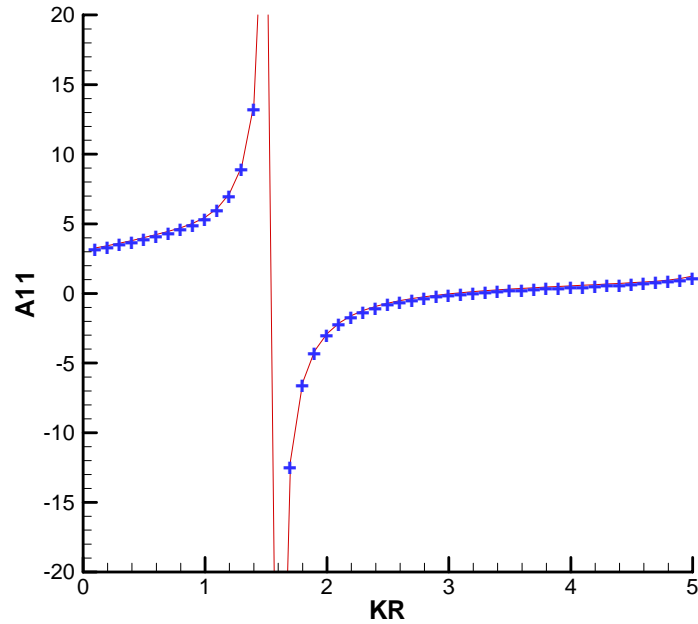
# Surge Internal

(normal reversed from External problem)



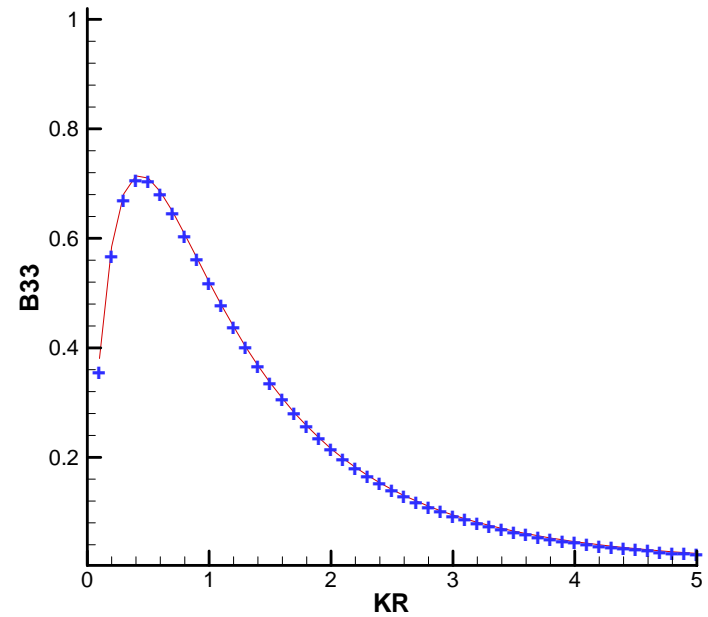
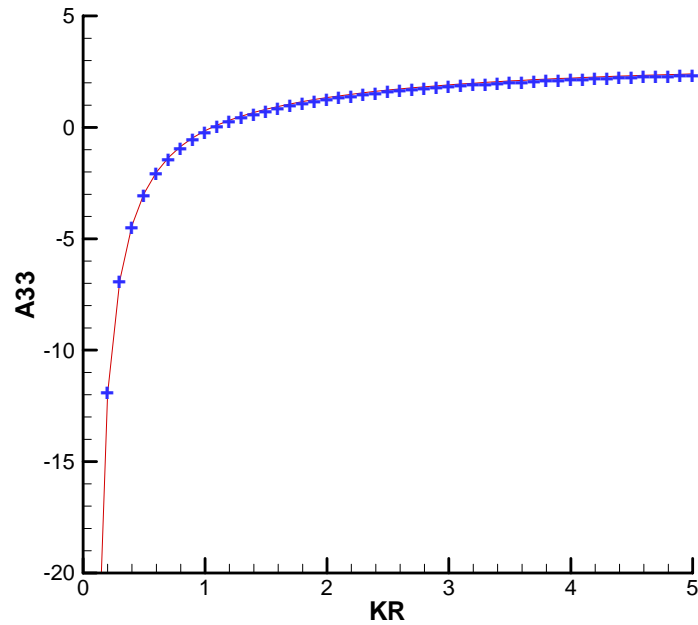
Sloshing effect near  $KR=1.6$  and 5

# Surge combined



Lines : external + internal  
Symbols:dipole surfaces

# Heave combined



Lines : external + internal  
Symbols: dipole surface



---

# Summary

- Thin structures can be analysed by the low-order method or higher order method.
  - In the higher order method, the hyper-singular integral is evaluated by numerical quadratures using the tangential plane on which  $dX/du = \text{constant}$ .
  - The higher-order method is more accurate especially for the small pressure jump on the dipole surface.
  - The results are not accurate for non uniform mapping. It is desirable to develop refined algorithms.
-

---

## Summary continues

- The accuracy of the higher order method indicates the fluid velocity on the body surface can be evaluated directly from the derivative of Green's equation (potential formulation).
  - Dipole surfaces may be used to analyse two regions separated by thin structures or membranes, but difficulty may arise due to internal resonances.
-

---

# Updates in V6.2

---

- F2T is provided as a separate program along with WAMIT V6.2. F2T converts the outputs of WAMIT into IRFs using Fourier transforms. (See F2T Manual appended in the report)

a) TEST14A.CFG:

.  
.  
**IPERIO=2**

b) TEST14A -- ISSC TLP (ILOWHI=1)

450  
0 0 IRAD, IDIFF  
**-101 NPER (array PER follows)**  
**-0.05 0.05 Initial, increment**  
1 NBETA (array BETA follows)  
0.  
1 NBODY  
test14.gdf  
0. 0. 0. 0. XBODY  
1 0 1 0 1 0 IMODE(1-6)  
0 NEWMDS

- 
- Zero and infinite frequencies for all output:

In addition to the added mass and damping (Option 1), the pressure and the fluid velocity on the body surface (Option 5) and at the field points (Options 6 and 7) can be evaluated for the zero and infinite wave frequencies.

- $IRR > 0$  and  $PER \leq 0$  :

Irregular frequency removal option can be specified for zero and infinite frequencies. In the previous versions, zero and infinite frequencies can not be run with irregular frequency removal option which includes the interior free surface as the computational domain.

---

---

- FGR0I2 replaces FGR0I1:

These subroutines evaluate Rankine source in two parallel horizontal walls and new version is extended to calculate double spatial derivatives

- Separate components of the hydrodynamic pressure and velocity at the field points due to the radiation modes and the diffraction field can be output separately. (Useful for post-processing when the dynamics of the body are modified)

In CFG:

INUMOPT6=0 total pressure in OUT / total pressure in .6

INUMOPT6=1 total pressure in OUT / components in .6

INUMOPT7 controls the velocity in .7x, 7y and 7z

---

---

- Dipole patches:

In the higher-order method, some or all of the body surface can be defined to represent thin structures

- TEST21.GDF SPAR2 with three strakes IGDEF=-12

18. 9.80665 ULEN GRAV

0 0 ISX ISY

7 -12 NPATCH IGDEF

**npatch\_dipole = 3**

**ipatch\_dipole = 2 4 6**

5

18. 200. RADIUS, DRAFT

3.7 0. 1. 3 WIDTH, THICKNESS, TWIST, NSTRAKE

0 IRRFRQ

0 0. IMOONPOOL, RADIUSMP

0 IMPGEN

---

---

## 2<sup>nd</sup>-order module

- The quadratic forcings are evaluated using Gauss quadrature. Rankine influences are evaluated and stored for all nodes for self-influence integrals and subdivisions. They are retrieved inside the 2<sup>nd</sup>-order frequency loops.
  - Free surface patches can be described in a similar manner as the body geometries using exact descriptions or MS2 files.
-



Application of generalized modes for the  
simulation of free surface patches in  
multiple body interactions

By J. N. Newman

- Resonant interactions can occur in the gap between two hulls, similar to pumping modes in moonpools but with variation of the amplitude along the length attenuating to near zero at the (open) ends of the gap. (Ref Newman & Sclavounos, BOSS `88)
- Linear potential theory generally overpredicts the amplitude of the resonances, which may be damped significantly by separation at the bilges, etc.
- As with pumping modes, an effective way to apply a semi-empirical damping factor in WAMIT can be implemented by adding a `lid' on the free surface. A sufficient number of generalized modes must be used to represent the longitudinal variation of the free surface.
- It is not necessary to completely cover the width of the gap, which simplifies the analysis.

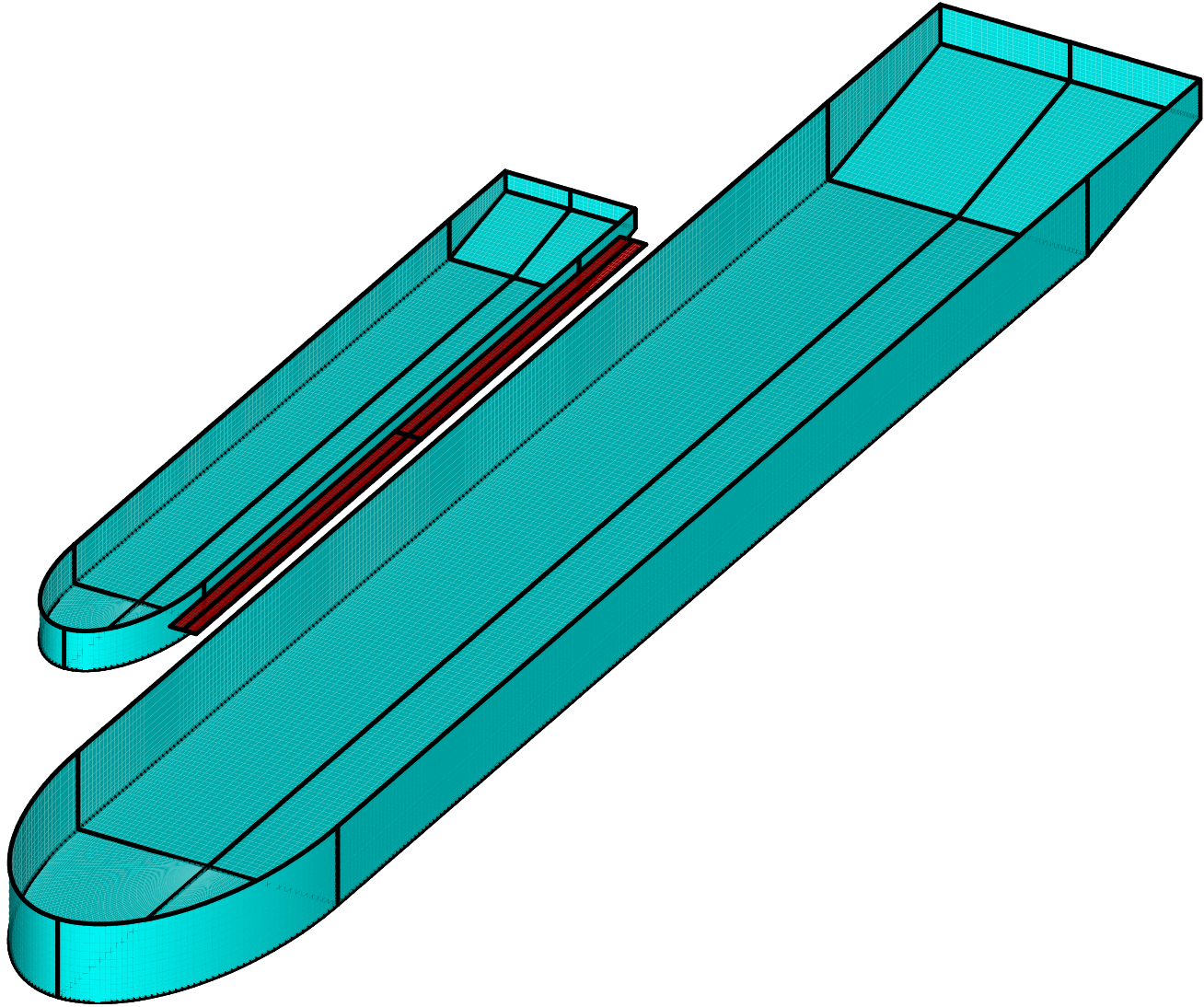
# Example used to test the method

- Two FPSO hulls: (a) 270m x 40m x 12m  
(b) 135m x 20m x 6m  
Gap width = 8m

Lid is a `barge' 120m x 4m x 0m

Generalized modes: Chebyshev

polynomials ( $n=0,1,\dots,15$ )



# Verification of method without damping

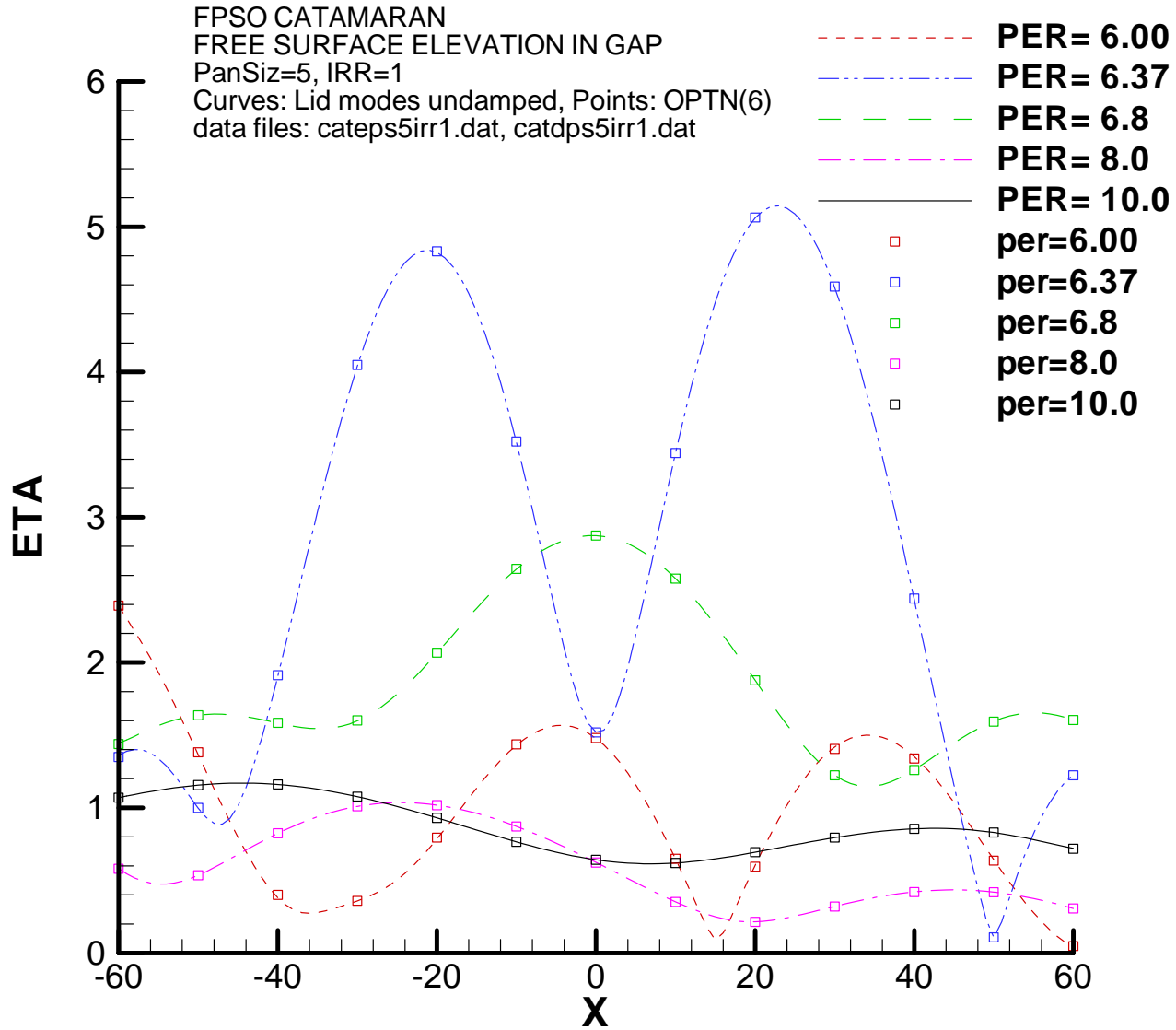
- The following plot compares the undamped lid amplitude derived from the generalized mode RAO's with the physical free surface amplitude computed without a lid (IOPTN 6) at five wave periods.
- The results are practically identical.

FPSO CATAMARAN  
FREE SURFACE ELEVATION IN GAP

PanSiz=5, IRR=1

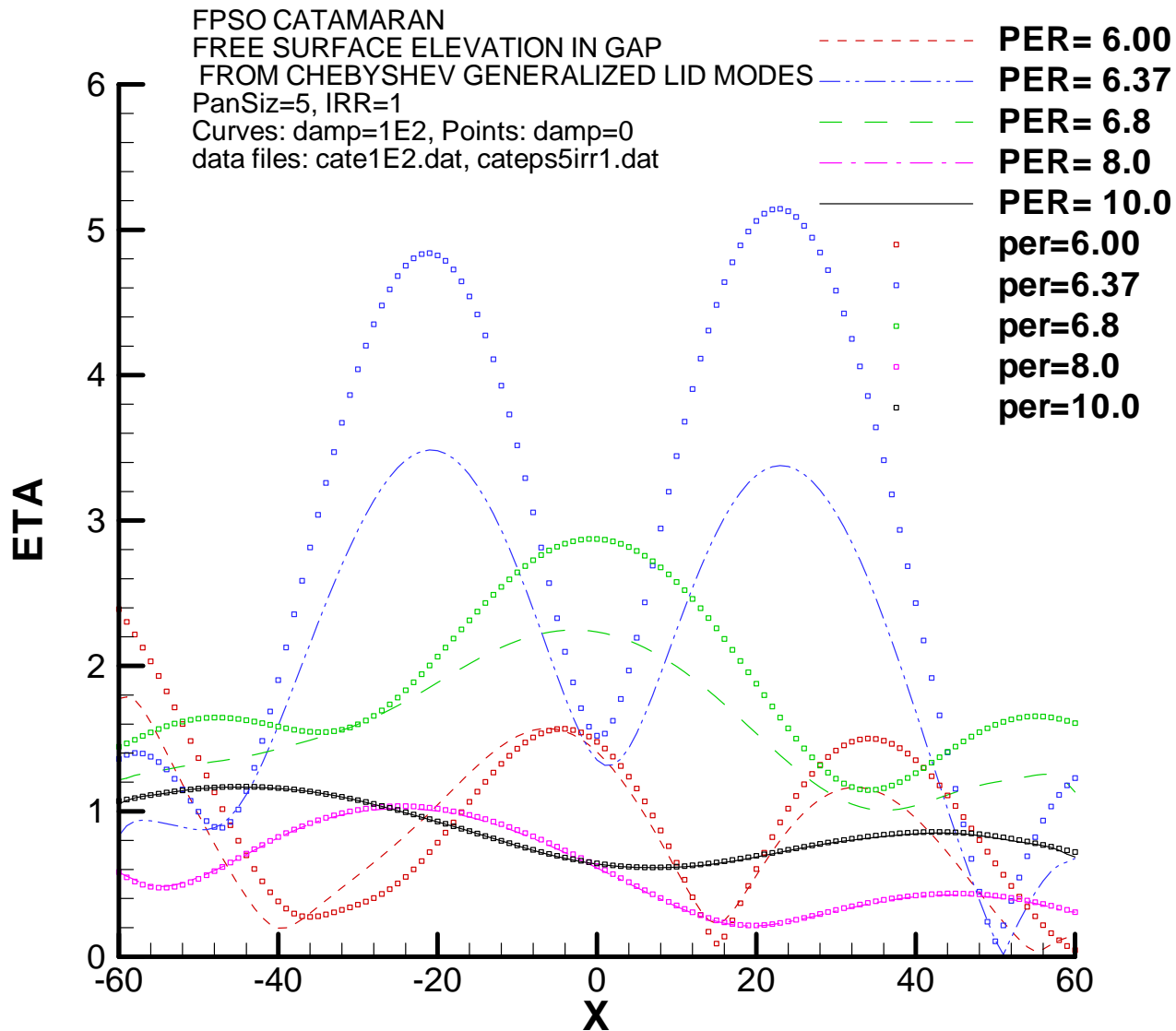
Curves: Lid modes undamped, Points: OPTN(6)

data files: cateps5irr1.dat, catdps5irr1.dat



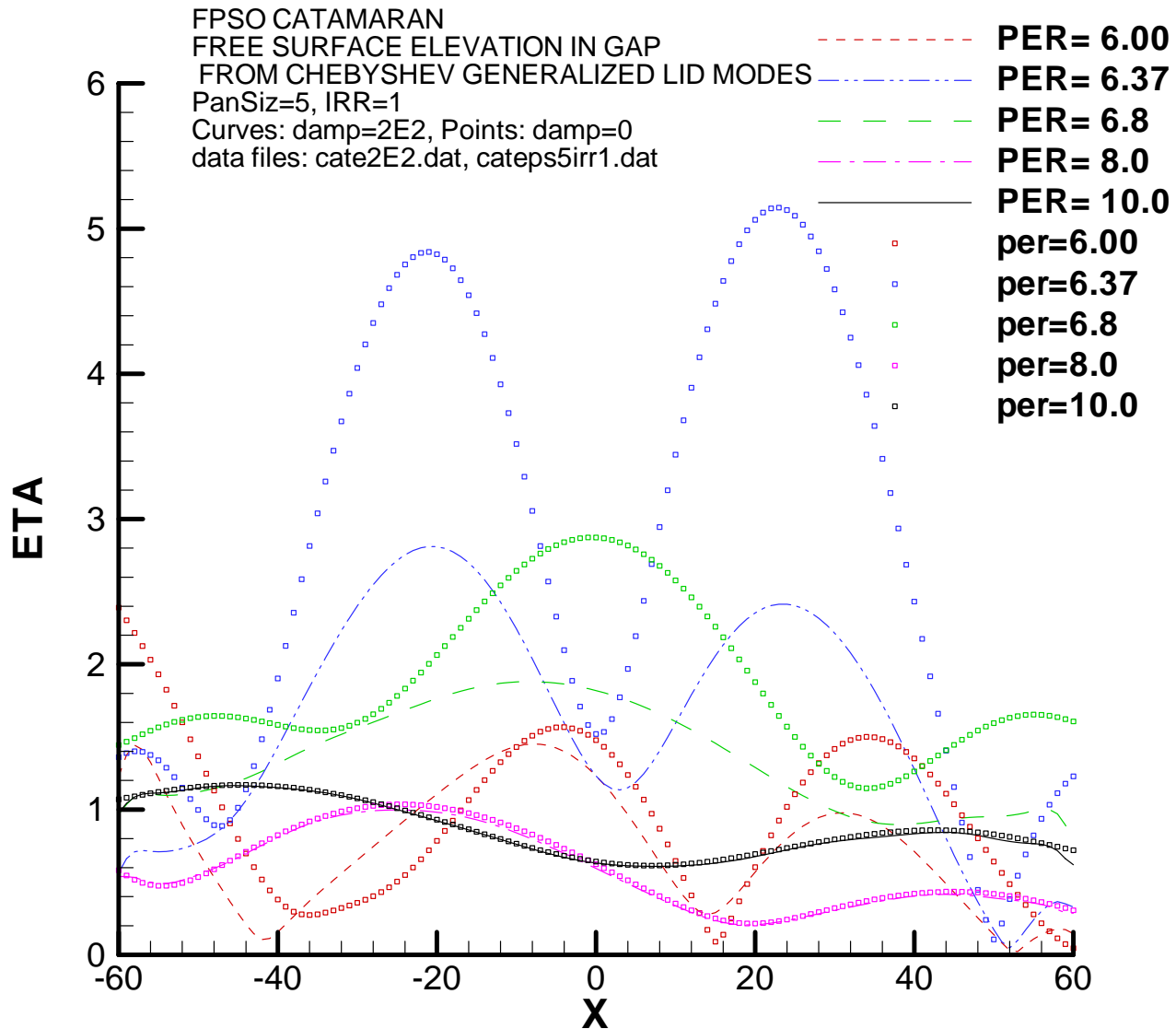
# Effect of external damping

- The following four plots show the lid motions with different external damping coefficients applied equally to all of the generalized modes.
- The undamped results are indicated by symbols for comparison.

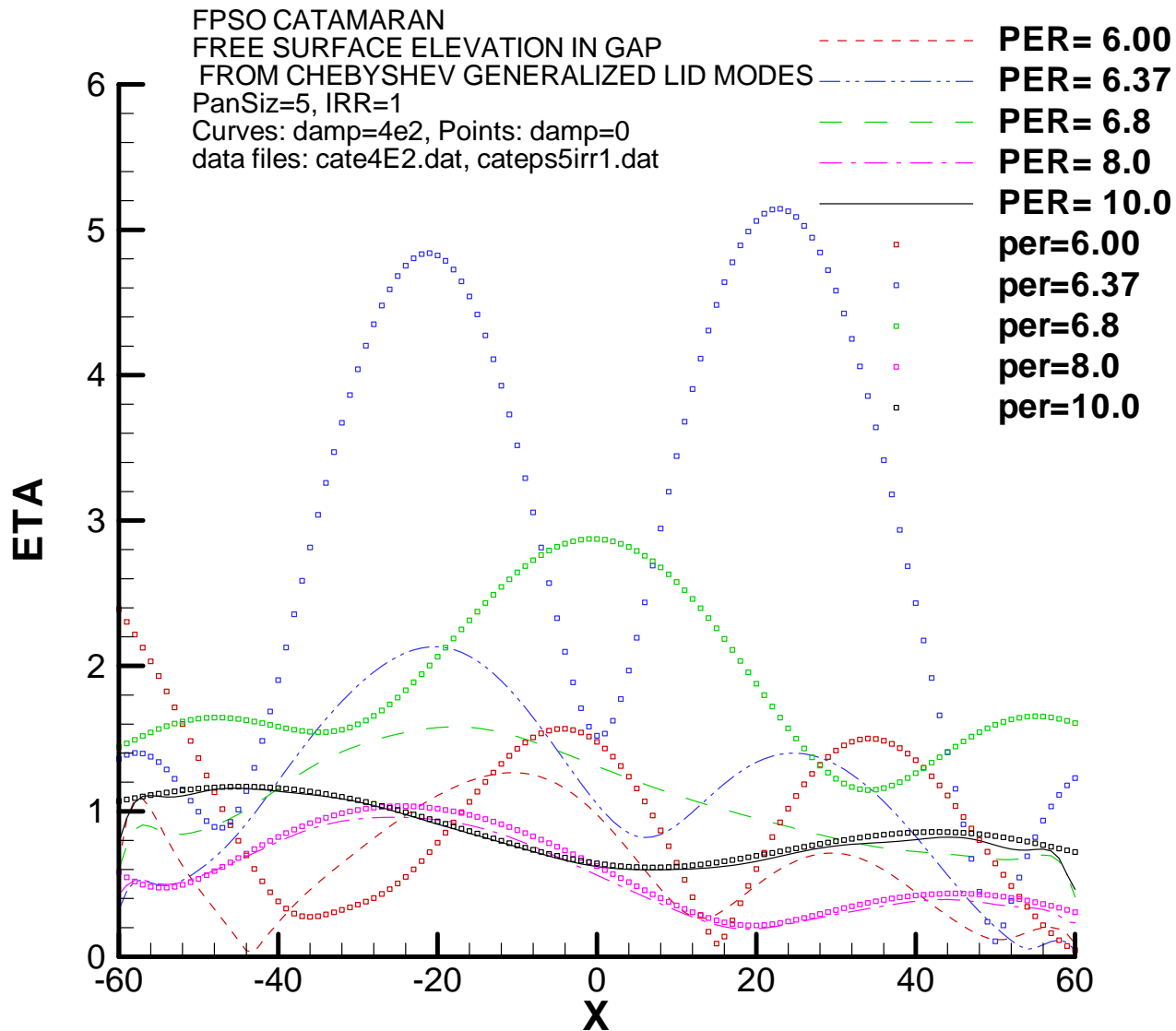


Damping = 100

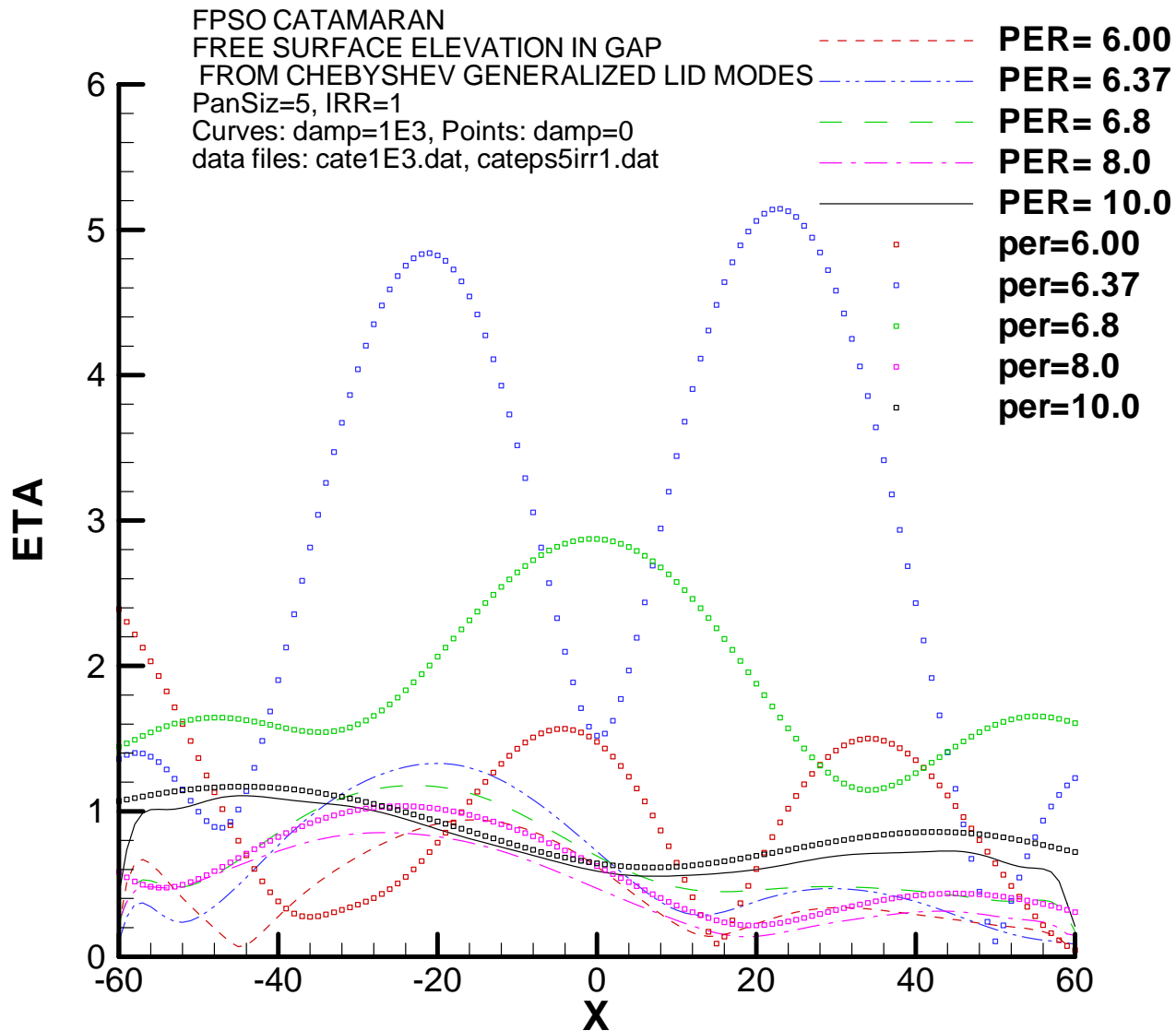




Damping = 200



Damping = 400



Damping = 1000

# Conclusions

- The method appears to work as intended. With moderate choices of damping the resonant modes are attenuated, with minimal effect on the free-surface amplitude at higher wave periods.
- It would be very interesting to compare similar results with experiments.

# Computational notes

- IRR=1 and PANEL\_SIZE=5 were used for most results. IRR=0 and/or PANEL\_SIZE=10 produced only small changes, on the order of 0.1
- A modified GEOMXACT subroutine FPSO12 was used to permit inputting different dimensions with the same subroutine. BARGE was used for the lid.

---

# Integration of second-order forcing in the higher-order method

---

$$2\pi\phi(\mathbf{x}) + \iint_{S_b} \phi G_{n_\xi} dS_\xi = \iint_{S_b} q_b(\omega_i, \omega_j) G dS_\xi + \iint_{S_f} q_f(\omega_i, \omega_j) G dS_\xi$$

- Frequency dependent second-order forcing is difficult to integrate efficiently in the higher-order method, because of the evaluations of Rankine influence for each frequency pair.
- In the low-order method, the forcing is assumed constant over each panel and the Rankine influences with constant source or dipole strengths are evaluated once and retrieved in the frequency loop.

---

## Higher-order method

### HIPAN-S

An attempt was made to fit the forcing in terms of B-splines. Rankine source, dipole and their higher moments are evaluated once and retrieved for the product with B-spline coefficients of the forcing in the frequency loop.

### V6.1S

Forcing are evaluated on the exact surfaces. But when it is integrated, the body and free surface are approximated with flat panels and the integration is carried out in piecewise manner as in the low-order method.

---



---

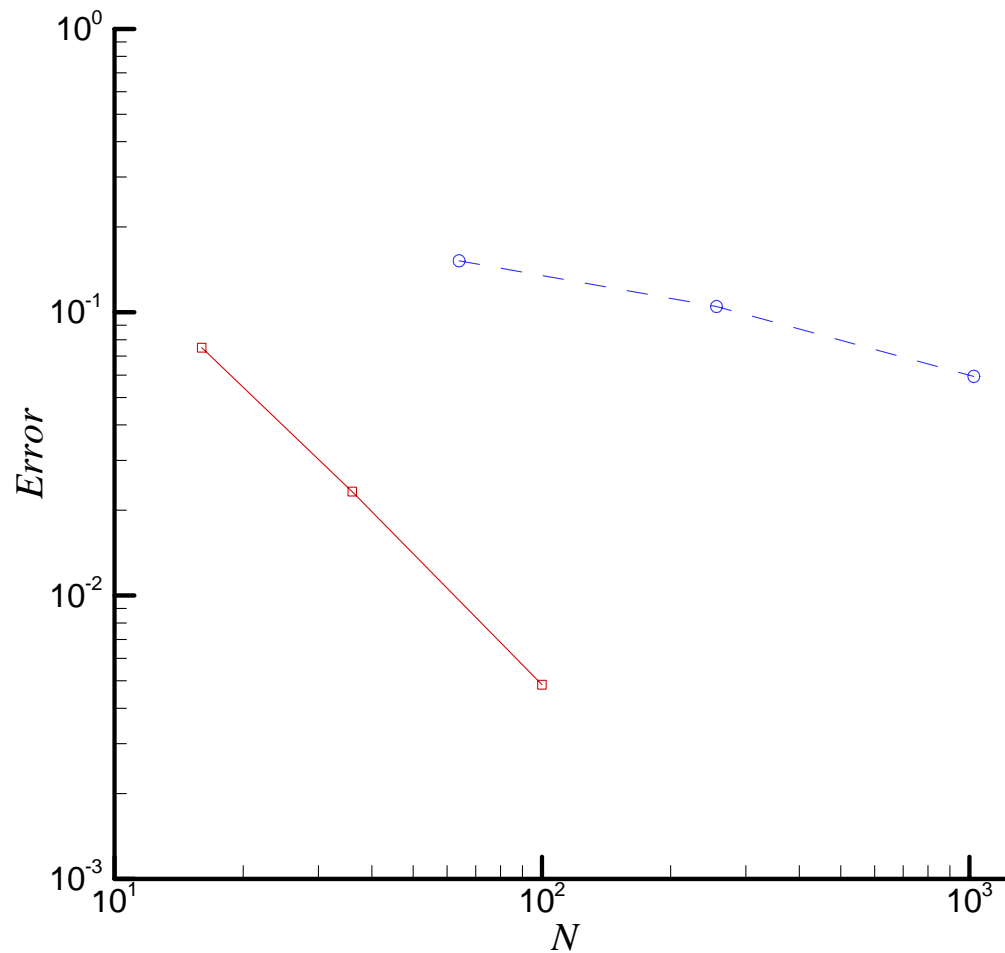
## ■ V6.2S

The nodes of Gauss quadrature including the self-influence and subdivisions are stored and retrieved in the frequency loop. Thus the forcing must be evaluated at all of these nodes.

Pro: Most accurate and robust

Con: Expensive for small problem

---



**2<sup>nd</sup> -order potential force**

Bottom mounted cylinder  
Radius=1, Draft=1, KR=1

Error is the difference with the semi-analytic solution 1.6398 (Newman,1996)

- 
- V6.2S has a new option for the integration of the forcing using Gauss quadrature in a very accurate manner.
  - Number of additional nodes due to the self influence and subdivision is  $O(100-1000)$  for each node of outer integral. It may be expensive for small number of unknowns.
  - Intersection between the body and free surfaces should be described accurately. The input free surface patches can be described using MS2 file or exactly as in GEOMXACT.
-

---

# Computation of the fluid velocity

---

---

## Low-order method

- Direct evaluation from the derivative of potential formulation is not accurate.
  - Velocity is evaluated based on the source formulation which has less singular kernel.
  - Velocity is not accurate except at the centroids on the body surface and in the vicinity of the panels in the fluid.
  - Quadratic pressure is less accurate than linear pressure. Non-uniform discretization toward the corners and waterlines somewhat improves the convergence. Generally it requires large number of panels for the bodies with corners.
-

# Higher-order method – current approach

- On the body surface, the velocity is evaluated from the derivatives of the velocity potential in the form

$$\nabla_{\mathbf{x}}\phi = \frac{\partial\phi(\mathbf{u})}{\partial\mathbf{u}} \cdot \frac{\partial\mathbf{u}}{\partial\mathbf{x}}$$

- Available at any points on the surface
- Simple to evaluate and very accurate on smooth surfaces
- In the fluid domain, the velocity is evaluated from the derivative of the potential formulation. Unlike the low-order method, it is accurate close to the body surface

---

## Despite the advantages in the previous page

- Geometric models should be created carefully so that the mappings do not have  $du/dx=0$  or  $dx/du=0$  except when such mappings are necessary to represent the local flow. For example, when a body has sharp corners, the mapping should be carefully chosen to have appropriate singularity corresponding to the corner flows.
  - But this is cumbersome and sometimes it is difficult to find appropriate mapping for complicated geometries.
  - **Thus it is desirable to compute velocity not affected strongly to the choice of mapping.**
-

# Higher-order method – New approach

- Evaluate the velocity from the derivatives of the potential formulation.

$$2\pi \nabla_s \phi(\mathbf{x}) + \iint_{S_b} \phi \nabla_s G_{n_\xi} dS_\xi = \iint_{S_b} \phi_{n_\xi} \nabla_s G dS_\xi \quad (\text{tangential})$$

+

$$4\pi \phi_n(\mathbf{x}) + \iint_{S_b} \phi G_{n_\xi n_x} dS_\xi = 2\pi \phi_n(\mathbf{x}) + \iint_{S_b} \phi_{n_\xi} G_{n_x} dS_\xi \quad (\text{normal})$$

||

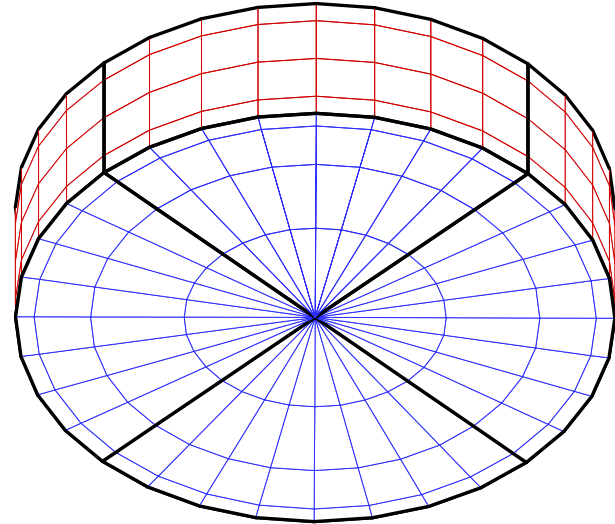
$$2\pi \nabla \phi(\mathbf{x}) + \iint_{S_b} \phi \nabla G_{n_\xi} dS_\xi = \iint_{S_b} \phi_{n_\xi} \nabla G dS_\xi$$

- The singular integrals are evaluated using the same method developed for the dipole patches



# Computational example

- Surge mean drift force on a freely floating cylinder ,  $R=1$  and  $T=0.5$ .
- 5 different levels of panel subdivisions from  $2 \times 1$  (24 unknowns) to  $32 \times 16$  (1124 unknowns) on each of two patches on a quadrant.

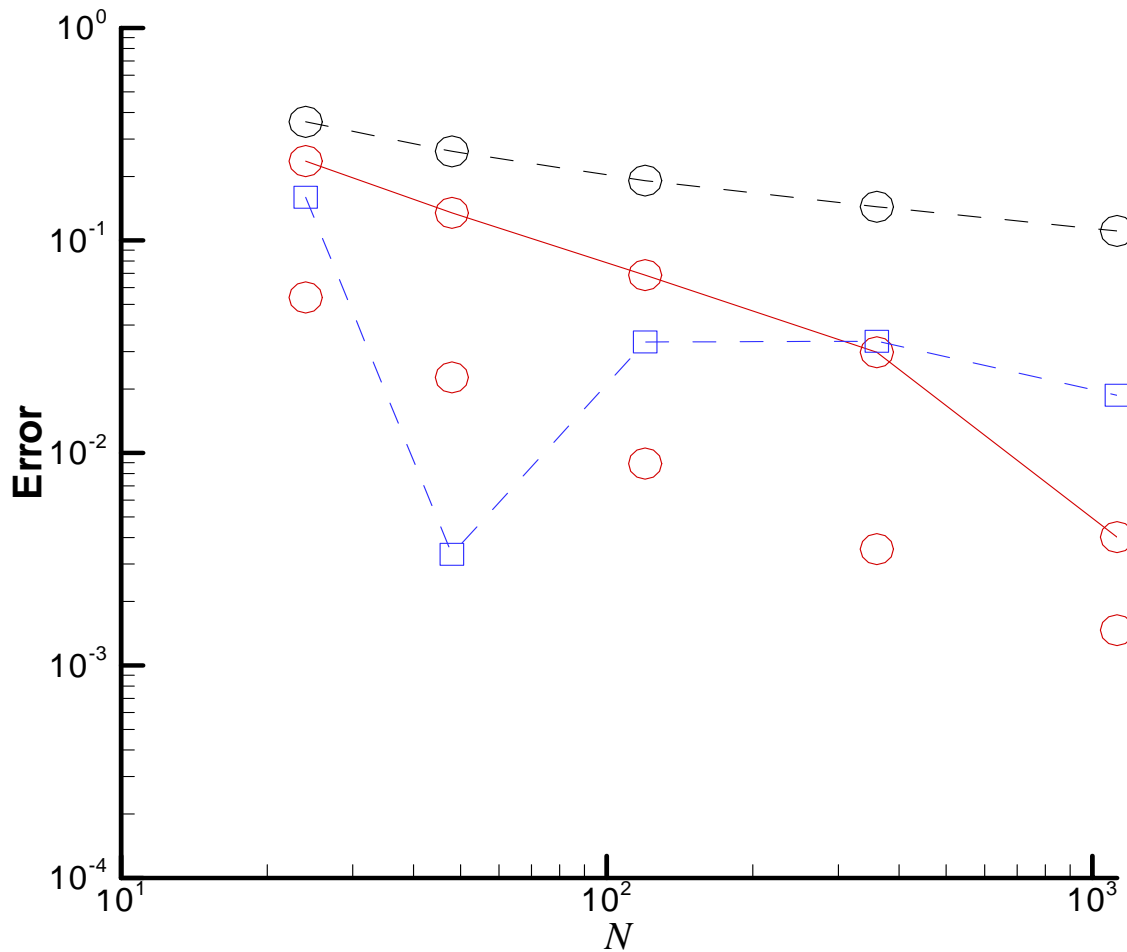


It shows medium subdivision  
 $8 \times 4$

---

# Computation notes

- Uniform mapping is used for the new approach (non uniform mapping can be handled accurately at present.)
  - Uniform and non-uniform mapping are used for the current approach in WAMIT (i.e. derivatives of the solution)
  - In all computation, the quadratic pressure is integrated using Gauss quadrature.
-




---

Line +symbol: pressure  
 Symbol only: momentum

uniform v6.2

non-uniform v6.2

uniform new

uniform momentum

Error is the difference with momentum drift force with non-uniform mapping  
 Among 3 drift forces by pressure integral, new approach is the most consistent  
 and converges faster than the other two for large  $N$ .

---

---

## Summary

- Preliminary result indicates the velocity can be evaluated directly from the potential formulation in the higher order method accurately. It is less sensitive to the mapping in comparison with current approach.
  - Increased computational time for the evaluation of the derivative of the kernel.
  - Need to develop robust algorithms for the self influence for non-uniform mapping.
-

---

# Updates in the pFFT method in WAMIT

---

# Review of pFFT

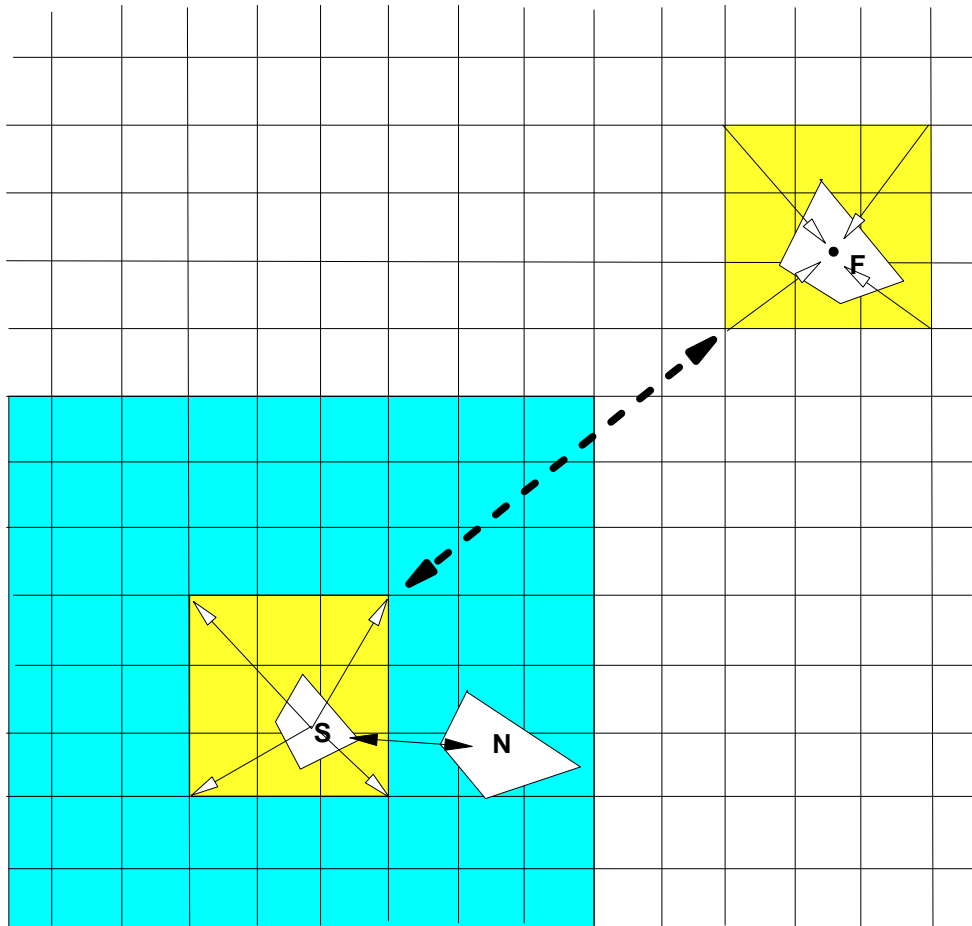
Seek solution by iterative method

$$D(\mathbf{x}, \boldsymbol{\xi})\phi(\boldsymbol{\xi}) = f(\mathbf{x})$$

$$(D_n + D_f)\phi = f$$

$$D_f\phi = I(\mathbf{x}, \mathbf{x}_g)C(\mathbf{x}_g; \boldsymbol{\xi}_g)P(\boldsymbol{\xi}_g, \boldsymbol{\xi})\phi(\boldsymbol{\xi})$$

$D$  is full matrix containing normal dipole influence coefficients. It is divided into near- and far-field elements. The product with far-field elements are carried out indirectly through the steps denoted by projection ( $P$ ), convolution ( $C$ ) and interpolation ( $I$ ). Each step represent a product of matrix and solution vector.



$$\phi(\xi_g) = P(\xi_g, \xi)\phi(\xi)$$

$$\phi(\mathbf{x}_g) = C(\mathbf{x}_g; \xi_g)\phi(\xi_g)$$

$$f'(\mathbf{x}) = I(\mathbf{x}, \mathbf{x}_g)\phi(\mathbf{x}_g)$$

$P$  represents the projection from panel (S) to grids

$C$  represents the interaction between grids

$I$  represents the interpolation from grid to panel (F)

$$\iint_{\text{panel}_j} G_{n_\xi}(\mathbf{x}; \boldsymbol{\xi}) dS_\xi = \sum G(\mathbf{x}; \boldsymbol{\xi}_g) P_j^T(\boldsymbol{\xi}_g)$$

$$C\phi_g = F^{-1}[F(C_1)F(\phi_g)]$$

$$G(\mathbf{x}; \boldsymbol{\xi}_i) = \sum G(\mathbf{x}; \boldsymbol{\xi}_g) I_i(\boldsymbol{\xi}_g)$$

***P*** and ***I*** are sparse matrices because only the near-by grids are considered. The product with these matrices is  $\mathcal{O}(N)$ . The product with ***C*** can be made in  $\mathcal{O}(N)$  using FFT.



- 
- Various refinements are made in the pFFT in WAMIT to improve the efficiency, primarily by the effective use of RAM and minimizing the access to hard disc.
  - $\frac{1}{4}$  M panels could be analysed with 1GB RAM. The required size of RAM is linearly proportional to the number of panels.
-

---

# Illustration

Arrays of cylinder  $R=11.5\text{m}$ ,  $D=20\text{m}$ , horizontal spacing  $40\text{m}$ .

Largest arrays has 2500 cylinders (100 x 25) and covers area  $4\text{km} \times 1\text{km}$

Horizontal mean drift force is computed and compared with box type structure of the same horizontal dimension and volume.

---

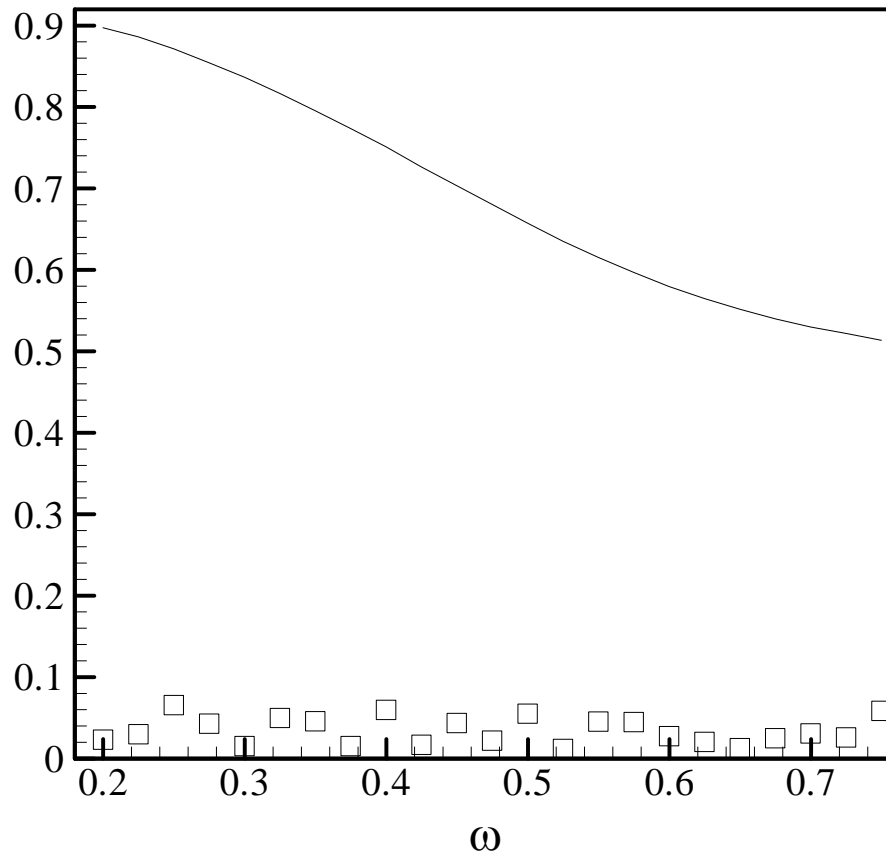
---

Computational time is linearly proportional to the number of unknowns (panels)

number of cylinders	number of unknowns	time per iteration
20 by 5	9600	0.2
36 by 9	31104	0.8
60 by 15	86400	3.4
100 by 25	240000	7.6

Table 1: The size of the linear system and the computational time required for one iteration, based on pFFT method. The CPU time is measured in seconds on a PC with a 1GHz Pentium processor.

---



Mean drift force on largest array (symbol) and box (line), normalized by the product of water density, gravity, wave amplitude square and half length.

- 
- Large problems can be analysed on PCs by the pFFT method
  - CPU per iteration (matrix-vector product) is small but the number of iterations varies significantly, from 16 to 400, depending on the wave period. It takes 7 seconds for the product of matrix-vector of dimension 240K, excluding times for the grid set-up and evaluation of the influences of near-by panels.
  - The pFFT method can be applied very effectively to the evaluation of the interaction between body and free surface panels in the 2<sup>nd</sup>-order problem. The interaction can be represented as a matrix-vector product which can be calculated by the same approach in the pFFT method.
-

## Current Participants

Chevron

Conoco

Norsk Hydro

OTRC

Petrobras/  
USP

Shell

Statoil

## Marcos Ferreira

Petrobras  
Cenpes-Diprex-Sedem  
Cidade Universitaria Quadra 7  
21949-900 Ilha do Fundao  
Rio de Janeiro, Brazil  
[marcos@cenpes.petrobras.com.br](mailto:marcos@cenpes.petrobras.com.br)

## Tim Finnigan

ChevronTexaco Exploration and Production Technology Co.  
6001 Bollinger Canyon Road  
Room L-4296  
San Ramon, CA 94583-2324  
[TimFinnigan@ChevronTexaco.com](mailto:TimFinnigan@ChevronTexaco.com)

## George Gu

Conoco  
NS 3052, Deep Water, EPT  
600 North Dairy Ashford  
Houston, TX 77079  
[george.z.gu@conocophillips.com](mailto:george.z.gu@conocophillips.com)

## Kjell Herford

Norsk Hydro ASA	Street Address
PO Box 7190	Sandsliveien 90
N-5020 Bergen, Norway	N-5254 Sandsli, Norway
<a href="mailto:Kjell.Herfjord@hydro.com">Kjell.Herfjord@hydro.com</a>	

## Kazuo Nishimoto

University of Sao Paulo  
Department of Naval Architecture and Ocean Engineering  
2231, Av. Prof. Mello Moraes  
Cidade Universitaria  
Sao Paulo, SP, Brazil CEPO05508-900  
[knishimo@usp.br](mailto:knishimo@usp.br)

## **Stergios Liapis**

Shell Oil Company  
Offshore Structures  
3737 Bellaire Blvd.  
Houston, TX 77025  
[sliapis@Shell.Com](mailto:sliapis@Shell.Com)

## **Rick Mercier**

Offshore Technology Research Center  
1200 Mariner Drive  
College Station, TX 77845-3400  
[rmercier@civilmail.tamu.edu](mailto:rmercier@civilmail.tamu.edu)

## **John Niedzwecki**

Offshore Technology Research Center  
1200 Mariner Drive  
College Station, TX 77845-3400  
[john@civilmail.tamu.edu](mailto:john@civilmail.tamu.edu)

## **Per Teigen**

STATOIL  
Postuttak  
N 7005 Trondheim  
Norway  
[pte@statoil.com](mailto:pte@statoil.com)

Street Address  
Ark, Ebbels v.10  
Rotvoll  
Trondheim, Norway

## **John Letcher**

AeroHydro  
54 Herrick Road/PO Box 684  
Southwest Harbor, ME 04679-0684  
[jletcher@aerohydro.com](mailto:jletcher@aerohydro.com)

## **Michael Shook**

AeroHydro  
54 Herrick Road/PO Box 684  
Southwest Harbor, ME 04679-0684  
[mshook@aerohydro.com](mailto:mshook@aerohydro.com)



## Michael Graham

Dept. of Aeronautics  
Imperial College  
London, SW7 2BY  
United Kingdom  
[m.graham@imperial.ac.uk](mailto:m.graham@imperial.ac.uk)

## Nick Newman

WAMIT  
1 Bowditch Road  
Woods Hole, MA 02543  
[jnn@mit.edu](mailto:jnn@mit.edu)

## Chang-Ho Lee

WAMIT  
822 Boylston Street, Suite 202  
Chestnut Hill, MA 02467  
[chlee@wamit.com](mailto:chlee@wamit.com)

## 2004 Meeting

Wed. Oct 6 - Thurs. Oct 7

# Appendices

# **F2T – A Fortran utility to evaluate time-domain impulse-response functions from WAMIT output (VERSION 3)**

by: J. N. Newman  
WAMIT, Inc., [www.wamit.com](http://www.wamit.com)

October 5, 2003

## **1 Introduction**

The Fortran utility F2T (Frequency-to-Time-domain) is a post-processor to transform frequency-domain WAMIT output to time-domain impulse-response functions (IRFs). This program is intended to provide a robust utility which can be used for general purposes, based on standard WAMIT outputs. This program accepts as input all of the first-order (linear) outputs from WAMIT, including any combinations of Options 1-7 (added mass/damping, Haskind exciting forces, Diffraction exciting forces, RAO's, body pressures/velocities, field-point pressures/velocities). In principle there are no restrictions regarding the numbers of rigid-body modes, generalized modes, or bodies. The computed IRFs are saved in output files which are analogous to the input files for each option and use the same filename extensions.

The Fourier transforms from the frequency-domain to the time-domain are evaluated in F2T by Filon numerical integration. This method provides relatively accurate results for large values of the time variable  $t$ . A fundamental requirement is that the frequency-domain data must be evaluated by WAMIT for a large number  $N$  of uniformly-spaced frequencies  $\omega_n$  where  $n=1,2,3,\dots,N$ . Special attention is necessary to ensure that the increment  $\Delta\omega = \omega_{n+1} - \omega_n$  is sufficiently small (to preserve the accuracy of the numerical integration) and that the highest finite frequency  $\omega_N$  is sufficiently large to span the physically-significant range of frequencies for the application (or from the mathematical standpoint, to ensure that the truncated Fourier integrals are reasonable approximations of the infinite integrals). In view of the need to include high frequencies in the WAMIT analysis it is usually advisable to use the irregular-frequency option (IRR=1), unless the body is submerged or its waterplane area is very small. The requirement of accuracy over a broad range of frequencies means that either a large number of low-order panels should be used, or alternatively that the higher-order method is used with appropriate control of the panel subdivision indices NU,NV or the global parameter PANEL\_SIZE.

## 2 Definitions of radiation and diffraction outputs

The outputs from WAMIT and F2T are considered to be of either the radiation or diffraction type, depending on whether they are caused by forced motions in calm water or by incident waves, respectively. The simplest physical distinction between these two types is in terms of the incident wave amplitude: if the response is proportional to the wave amplitude it is of the diffraction type, and vice versa.

The added-mass and damping coefficients (Option 1) are of the radiation type, whereas the exciting forces and RAO's (Options 2,3,4) are of the diffraction type. Except as noted below, the pressures and fluid velocities on the body (Option 5) and in the fluid (Options 6,7) are of the diffraction type, since these are defined in the WAMIT convention as total responses with the body free to respond (or fixed) in incident waves. There are two exceptions which affect the Options 5,6,7. If IDIFF=-1 is specified in the WAMIT run, signifying that there are no incident waves, the outputs from Options 5,6,7 are the total responses from superposition of all specified radiation modes; in this case all of the available outputs are of the radiation type. If the configuration parameters INUMOPT5, INUMOPT6, INUMOPT7 = 1 in the WAMIT run, the corresponding Option 5,6,7 outputs are separated into radiation components for each mode of forced motion plus the diffraction component, as explained in the WAMIT User Manual Sections 4.9 and 4.12 (Version 6.2); in this case F2T analyses the radiation components and diffraction components separately, according to their types.

A fundamental distinction between the two types of outputs is in terms of their limits at infinite frequency or zero period. In this limit the radiation outputs are generally real and nonzero, corresponding to the added mass, pressure, and fluid velocity induced by forced motions of the body without wave effects on the free surface. Conversely, in the same limit there are no diffraction effects since the 'incident waves' have vanishingly small wavelength and cause no disturbance of either the body or the fluid.

When radiation IRFs are evaluated it is necessary to evaluate the corresponding frequency-domain coefficients for  $\omega_0 = 0$  and  $\omega_{N+1} = \infty$ , using the special instructions in the WAMIT User Manual (Section 3.1, page 3-9 of the V6.1 User Manual). Thus, in V6.1, two WAMIT runs are required. V6.1 also restricts the  $\omega_0 = 0$  and  $\omega_{N+1} = \infty$  evaluations to Option 1, so that V6.1 cannot be used with F2T to analyse radiation type outputs in Options 5,6,7. Normally this will not be a restriction, except in cases where IDIFF=-1 or INUMOPT5=1 are used. WAMIT V6.2 removes this restriction, and will also permit the analysis of all frequency-domain outputs to be made in a single run. To simplify the instructions below, V6.2 is assumed and instructions are given for making only one WAMIT run. (Users of V6.1 should make two separate runs, one for finite wave periods and one for zero and infinity, and for the latter only Option 1 should be specified.)

## 3 Acquiring input data for F2T with WAMIT

The frequency-domain input data is evaluated by WAMIT, with the following special provision:

- A uniformly-spaced set of frequencies  $\omega_n$  should be defined in the .POT file, where  $\omega_n = n\Delta\omega$ , and ( $n=1,2,3,\dots,NPER$ ). This is done most easily by setting the parameter IPERIO=2 in the configuration file (inputs are radian frequencies), and by using the option to write the data -NPER and  $\omega_1$ ,  $\Delta\omega$  on the lines normally used to specify NPER and the array PER. The simplest procedure using V6.2 is to make one run, with  $\omega_1 = -\Delta\omega$ , so that

both infinite and zero wave periods are included in the run. (Note in this case that NPER must include the total number of wave periods including zero and infinity.)

The input files used for the tests of the ISSC TLP can be regarded as an example. These files are named IMPTLP.\*. They are essentially the same as for TEST14, with the exception of IPERIO=2 in TEST14.CFG, and infinite depth has been assumed to accelerate the test runs.

When the input files to F2T are read, the data is sorted so that the frequencies are listed in ascending order, regardless of their order in the WAMIT output files. Thus the order of the periods (-1.0, 0.0) is irrelevant, and it is possible to patch together two or more separate sets of output files from WAMIT, e.g. one with a coarse set of wave frequencies and the other with intermediate frequencies, to provide a finer set, without concern regarding their order.

## 4 How to use F2T

The program F2T can be executed after the appropriate WAMIT output files are available. The user must specify the filenames of these files and a small number of input parameters, either interactively in response to appropriate runtime prompts or by preparing the special input file `inputs.f2t`. The following example of this special input file corresponds to the IMPTLP example described above:

```
header line for inputs.f2t control file, TLP example
IMPTLP
0 0 1 (IRAD IDIFF NUMHDR)
0 0 0 (INUMOPT5 INUMOPT6 INUMOPT7)
0.2 100 (DT NT time step and number of time steps)
0 (IOUTFCFS, output both cosine and sine transforms)
```

These inputs are described for each line as follows:

Line 1 is an ASCII header dimensioned CHARACTER\*72 as in most WAMIT input files. This line should be used to insert a brief description of the file.

Line 2 is a list of the filenames (not the extensions) of the primary and secondary WAMIT output files. F2T attempts to open all numeric output files with the same filenames, and includes all of these files in the analysis. Thus the determination of which options to be included depends on the available WAMIT output files. In this example where the TEST14.FRC control file was used as in the standard WAMIT test runs, Options 1,2,3,4 will be included in the F2T analysis. If all of the input data is included in the primary file it is not necessary to list other filenames. Additional secondary files can also be included, up to a maximum limit of 256 ASCII characters for the complete line. At least one blank space must be used to separate each filename.

Lines 3 and 4 contain the six WAMIT control parameters identified by the comments in parenthesis. These parameters must have the same values as in the WAMIT runs. (No distinction is made between IRAD,IDIFF=0 or 1, and the only important value to specify correctly is -1. For any input values of IRAD,IDIFF other than -1 the results are the same as for 0 or 1.) NUMHDR, which is optional in WAMIT with the default value 0, must be specified here with the value 0 (no headers) or 1 (one line of headers) to indicate the presence or absence of a header line in the WAMIT numeric output files. INUMOPT5, the optional configuration parameter introduced in WAMIT Version 6.1 to permit outputting separate components of the

body pressure and velocity, and also INUMOPT6, INUMOPT7 introduced in Version 6.2 must be specified here with the value 0 (default in WAMIT) or the separate-components values 1.

Line 5 contains the time step and number of time steps for the computation and tabulation of the time-domain response functions. The radiation IRF'S are computed and tabulated for  $t=0$  and for NT positive times DT, 2DT, 3DT, ..., NT\*DT. The diffraction IRFs are evaluated for both positive and negative times, starting with  $-NT*DT$  and ending with  $+NT*DT$ .

Line 6 contains the optional parameter IOUTFCFS, with the following options for its value:

IOUTFCFS=1: output only the cosine transform of radiation irf's

IOUTFCFS=2: output only the sine transform of radiation irf's

IOUTFCFS=0 (or any other integer except 1 or 2): output both cosine and sine transforms (These transforms are redundant, as explained below.) The default value IOUTFCFS=0 is used if line 6 is missing from the file. Thus the use of this parameter is optional.

The use of the special file `inputs.f2t` is optional. If this file does not exist, or if the first five lines cannot be read with the appropriate data, the user is prompted to specify all of the above inputs interactively. The special file can also be used in a partial form with some but not all of the above lines, but the lines included must be in the same order as above. This permits the user to interactively input different values of the time step and number, simply by omitting Line 5 from the special file.

The numeric data in the special file is read with free format READ statements, separately for each line. Any additional text on the same lines is ignored, so that comments may be inserted as in the example above. The filenames on Line 2 are read as ASCII text of unknown length (maximum of 256 characters, all on one line) and no additional comments may be included on this line.

The output files from F2T are in two complementary formats with duplication of the output data in the two formats. The filename assigned to all of the output files is *primary*, with different extensions. The first set of output files have appended filenames including `_JR` followed by the same extensions as the WAMIT output files. The second set have the appended filenames including `_JR`. The first set follow the same format as the WAMIT numeric output files of the same number, except that the period is replaced by the time step and the WAMIT force coefficients are replaced by their Fourier cosine and sine transforms. Different modes and mode combinations are listed on separate lines with the identifying mode indices, just as in the numeric output files of WAMIT.

To facilitate plotting and separation of the different modes and wave angles (BETA), all of the Fourier cosine/sine transforms are listed on one line in the output files denoted by `_JR`, in the same order of mode combinations but without explicit mode indices. The cosine/sine transforms are listed as pairs, unless one or the other is omitted by setting IOUTFCFS equal to 1 or 2 as explained in the following paragraph. Column one of the `_JR` file contains the value of time  $t$ .

Either the cosine transforms of the added mass or the sine transforms of the damping can be used to evaluate the radiation IRFs (cf. equations 3 and 4 below). These two sets of data can be checked to verify their accuracy and consistency, in much the same way that the Haskind and Diffraction exciting forces or cross-coupling coefficients are compared. Alternatively, to achieve more compact output files, one of these transforms can be omitted using the parameter IOUTFCFS.

One more output file is produced with the extension `.KR1`, containing the impulse-response functions  $K_{ij}$  which are evaluated in TiMIT. These alternative IRF's are evaluated in F2T by

numerical differentiation of the IRF's  $L_{ij}$  which are defined below.

The diffraction files `_JR` are different from the radiation files in two respects, to facilitate their use. First, the time steps begin with  $-NT*DT$ , and end with  $+NT*DT$ . Secondly, the cosine and sine transforms are combined (adding for  $t < 0$  and subtracting for  $t > 0$ ) to give the actual IRFs for the corresponding exciting forces and RAOs (cf. equation 8 below).

For practical purposes the `.JRn` files will be most useful, and the `.IRn` files may be useful only to clarify the identity of the different columns in the `.JRn` files.

Some experience and/or trial computations will be needed to determine appropriate values of the input frequencies and time steps. The dimensions of these parameters correspond to GRAV in the WAMIT run.



## 5 Theory

The fundamental relations between the time- and frequency-domain express the added-mass coefficient  $A_{ij}$  and damping coefficient  $B_{ij}$  in terms of Fourier transforms of the impulse-response function  $L_{ij}(t)$ :

$$A_{ij}(\omega) - A_{ij}(\infty) = \int_0^\infty L_{ij}(t) \cos \omega t dt \quad (1)$$

$$B_{ij}(\omega) = \omega \int_0^\infty L_{ij}(t) \sin \omega t dt \quad (2)$$

The inverse-transforms of (1-2) give complementary relations for the impulse-response function:

$$L_{ij}(t) = \frac{2}{\pi} \int_0^\infty [A_{ij}(\omega) - A_{ij}(\infty)] \cos \omega t d\omega \quad (3)$$

$$L_{ij}(t) = \frac{2}{\pi} \int_0^\infty \frac{B_{ij}(\omega)}{\omega} \sin \omega t d\omega \quad (4)$$

Similar relations exist for the exciting forces and RAOs. Define one of these quantities by the complex function  $X_i(\omega)$ . The corresponding impulse-response function is real, denoted by  $K_i(t)$ . The appropriate physical ranges are  $(0 \leq \omega < \infty)$  and  $(-\infty < t < \infty)$ . Then the complex Fourier transform pairs are as follows:

$$X_i(\omega) = \int_{-\infty}^\infty K_i(t) e^{-i\omega t} dt \quad (5)$$

and

$$2\pi K_i(t) = \int_{-\infty}^\infty X_i(\omega) e^{i\omega t} d\omega \quad (6)$$

Formally, since  $K_i$  is real,  $X_i(-\omega) = X_i^*(\omega)$ , and thus

$$2\pi K_i(t) = \int_0^\infty [X_i(\omega) e^{i\omega t} + X_i^*(\omega) e^{-i\omega t}] d\omega \quad (7)$$

or

$$K_i(t) = \frac{1}{\pi} \int_0^\infty [\operatorname{Re}(X_i) \cos \omega t - \operatorname{Im}(X_i) \sin \omega t] d\omega \quad (8)$$

The principal task is to evaluate (3), (4), and (8). This is done by truncating the infinite integrations at the largest value of the evaluated frequency, and using Filon quadratures to evaluate the resulting finite integrals. A truncation correction is derived below, and applied to (3). (This correction is more robust than the correction which was described last year.)

Usually the most significant truncation error is associated with the transform of the added-mass (3). From partial integration of (1) it follows that

$$A_{ij}(\omega) - A_{ij}(\infty) = -\frac{1}{\omega} \int_0^\infty L'_{ij}(t) \sin \omega t dt \simeq -L'(0)\omega^{-2} \quad (9)$$

where the neglected integral is of order  $\omega^{-3}$ . If (3) is truncated at a finite frequency  $\omega_N = \Omega$ , the truncation correction is

$$\Lambda_{ij}(t) = \frac{2}{\pi} \int_\Omega^\infty [A_{ij}(\omega) - A_{ij}(\infty)] \cos \omega t d\omega \quad (10)$$

This can be approximated, using (9), if  $\Omega$  is sufficiently large:

$$\Lambda_{ij}(t) \simeq -\frac{2}{\pi} L'_{ij}(0) \int_{\Omega}^{\infty} \omega^{-2} \cos \omega t d\omega = -\frac{2}{\pi\Omega} L'_{ij}(0) [\cos \Omega t + \Omega t \text{si}(\Omega t)] \quad (11)$$

Here we follow the notation of Abramowitz & Stegun (equation 5.2.26) for the sine integral

$$\int_z^{\infty} \frac{\sin t}{t} dt = -\text{si}(z)$$

The constant  $L'_{ij}(0)$  can be evaluated from the fact that  $L_{ij}(0) = 0$ , and thus

$$\Lambda_{ij}(0) = -\frac{2}{\pi} \int_0^{\Omega} [A_{ij}(\omega) - A_{ij}(\infty)] d\omega \simeq -\frac{2}{\pi\Omega} L'_{ij}(0) \quad (12)$$

Combining (11) and (12) gives the truncation correction in (10) in the form

$$\Lambda_{ij}(t) \simeq -\frac{2}{\pi} [\cos \Omega t + \Omega t \text{si}(\Omega t)] \int_0^{\Omega} [A_{ij}(\omega) - A_{ij}(\infty)] d\omega \quad (13)$$

This is the procedure which was used last year, but it suffers from the slow algebraic convergence of the last integral. The new procedure, which is adopted in F2T, is based instead on differentiating (4) to give the relations

$$L'_{ij}(0) = \frac{2}{\pi} \int_0^{\infty} B_{ij}(\omega) d\omega \simeq \frac{2}{\pi} \int_0^{\Omega} B_{ij}(\omega) d\omega \quad (14)$$

$$\Lambda_{ij}(t) \simeq -\frac{4}{\pi^2\Omega} [\cos \Omega t + \Omega t \text{si}(\Omega t)] \int_0^{\Omega} B_{ij}(\omega) d\omega \quad (15)$$

Equations (12) and (14) are complementary, but (14) is more robust since the integrand of (14) is positive-definite and converges to zero more rapidly than the integrand of (12).